24th COBEM - 2017

24th ABCM International Congress of Mechanical Engineering
December 3-8, 2017, Curitiba, PR, Brazil

COBEM-2017-2055
CAVITATION EROSION RESISTANCE OF A Co28Cr22Fe ALLOY

Manuelle Curbani Romero
Juliana Lima Barbarioli
Federal University of Espírito Santo, Department of Mechanical Engineering, CTIII, Vitória, 29075-910, Brazil
manu.curbani@gmail.com; julianabarbarioli.1@gmail.com

André Paulo Tschiptschin
Metallurgical and Materials Engineering Department, University of São Paulo, Av. Prof. Mello Moraes 2463, 05508-030 São Paulo, Brazil
antschip@usp.br

Cherlio Scandian
Federal University of Espírito Santo, Department of Mechanical Engineering, CTIII, Vitória, 29075-910, Brazil
cherlio@hotmail.com

Abstract. *The aim of this study is to evaluate the cavitation erosion (CE) resistance of a nonstandard cobalt based alloy (Co28Cr22Fe) in three different conditions: as cast, solution treated and cold-worked. The main material removal operating mechanism was flaking at slip lines and at slip lines intersections. The cold-worked samples exhibited the best CE resistance and the solution treated the worst.*

Keywords: *Cobalt alloys, Cavitation Erosion, As cast, Solution treated, Cold-worked.*

1. INTRODUCTION

Cavitation erosion (CE) is a damaging process that very often impairs the performance of hydraulic equipments. When liquids undergo a localized pressure reduction below the vapor pressure, bubbles are formed (Jean, 2005). The implosion of these bubbles, when the pressure rises above the liquid vapor pressure, causes the formation of shock waves and increases local temperature, leading to erosion damage at the material's surface. Due to the progressive increase of operational pressures and speeds, aiming higher efficiency, CE damage is even more frequent, causing an increase in the repairing costs of the equipments (Hansson and Hansson, 1992).

Gould (1980) attributed the superior CE wear resistance of cobalt alloys to a strain-induced martensitic transformation, that consumes a large part of the cavitation energy. On the other hand, Vaidya and Preece (1978) reported that cobalt do not suffer a martensitic transformation, but, a fine-scale mechanical twinning. Several authors pointed the stacking fault energy (SFE) as the main parameter governing the CE resistance (Stoltz and Vander Sande, 1980; Vaidya et al., 1980). Materials as cobalt with a very low SFE, deforms by a planar slip deformation mechanism, which increases the numbers of cycles that would result in fatigue failure, considering that CE is a fatigue process (Richman and McNaughton, 1990).

Heathcock et al. (1982) and Romo et al. (2012) investigated wear mechanisms for Stellite alloys. They noted that the interfaces between carbides and the matrix were preferably eroded, Hattori and Mikami (2009) attributed this behavior to the presence of an extruded region on that interface – the carbide is harder than the matrix, leading to a different degree of plastic deformation. Mass removal occurred by carbide dislodge and later by flaking caused by fatigue cracks under the surface. Seedhar (2015), studying Stellite 6 coatings, observed that cracks were initiated due to work hardening of the matrix after prolonged testing.

Mills and Knutsen (1998) observed that cold-working of CrMnN alloys greatly improved the CE resistance, since it increases the yield strength and delays the material removal, which occurs in three steps: i. plastic deformation inside the grains; ii. plastic extrusion at grain boundaries; iii. fatigue damage at extruded grain boundaries. Mesa et al. (2010) corroborated this effect in a High Temperature Gas Nitrided (HTGN) UNS S31803 duplex stainless steels and added that the higher difficulty to create and move dislocations is combined with the reduction of toughness, that could make easier debris flaking.

The aim of this work is to investigate the effect of the solution treatment and cold-working on the CE resistance of Co28Cr22Fe alloy and investigate the operating wear mechanisms, as well.

2. EXPERIMENTAL PROCEDURE

The nominal chemical composition of Co28Cr22Fe is shown in Table 1. A set of 5 samples were solution treated at 1573K for 12 hours and quenched in water to obtain a FCC (Face-Centered Cubic) microstructure free from precipitates. Another set of 5 samples followed the same solubilization treatment and then were submitted to 30% cold-rolling.

Table 1. Co28Cr22Fe Chemical Composition

	Co	Cr	W	Mo	C	Fe	Si
Co28Cr22Fe alloy	Bal.	28	0.2	0.3	<0,15	22	<1.2

The specimens were tested in a Telsonic SG 1000, vibratory cavitation apparatus using the indirect method, according to ASTM G32 standard. Test conditions are listed in Table 2. Mass losses were periodically measured and their CE resistances were compared to AISI 304L. Prior to the tests, the samples were grounded and polished with diamond paste (6, 3, 1 μm).

The microstructure of the specimens was examined by optical microscopy and low-magnification stereo microscopy. Vickers microhardness was measured using 0,1 kgf load. The worn surfaces were analyzed by Scanning Electron Microscopy (SEM) trying to identify the material removal mechanisms.

Table 2. Vibratory CE test parameters

Frequency	20 Khz
Peak amplitude	40 μm
Separation between horn and sample	0.5 mm
Temperature	25 ± 2°C

X-ray diffraction (XRD) was used to characterize the crystal structure of the as cast and solution treated cobalt alloy.

3. RESULTS AND DISCUSSION

3.1 Microstructure characterization

Figure 1 shows the microstructure of the as cast Co28Cr22Fe alloy. The microstructure consists of coarse as-cast dendritic grains, with an average grain size of 2 mm. It is also possible to observe the presence of deformation twins inside the grains. A small fraction of carbides can be seen.

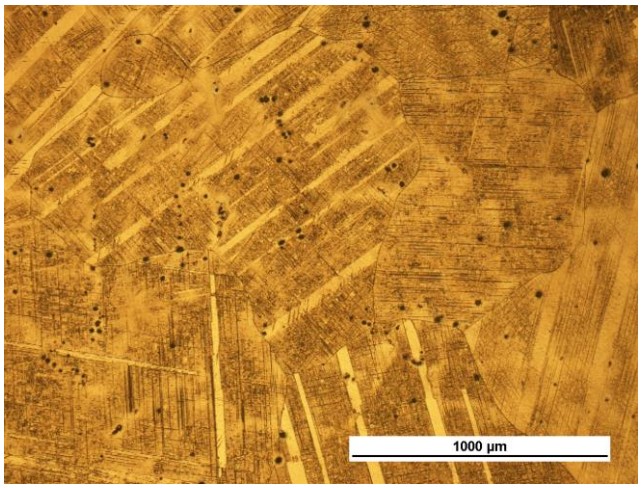

Figure 1. Optical micrograph - As cast Co28Cr22Fe alloy (100 ml HCl + 5 ml H_2O_2)

After the solution treatment, a primary recristallyzation occured. Figure 2 shows a bimodal distribution of grain sizes, small recrystallized grains aside 6 mm coarse grains, indicating that during the treatment, grain growth also occured. These new grains grew inside the coarse pre-existing as-cast grains. Several annealing twins can be seen inside the recrystallized grains, as shown in Fig. 3. The sample is almost free of precipitates.

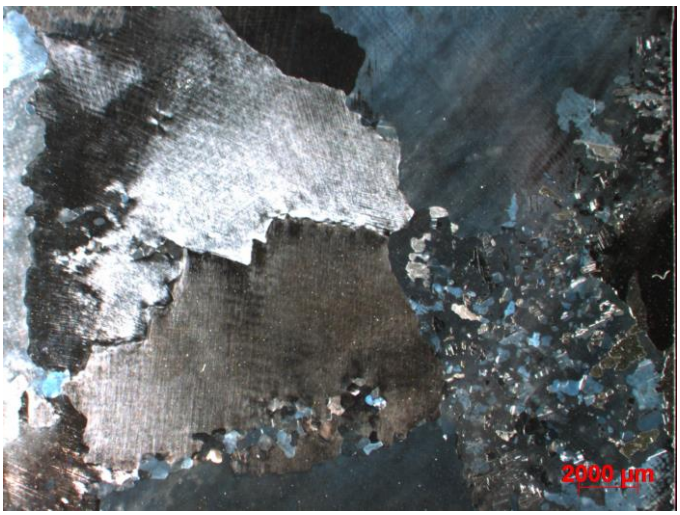

Figure 2. Stereoscopic optical image (5x) - Microstructure solution treated Co28Cr22Fe alloy

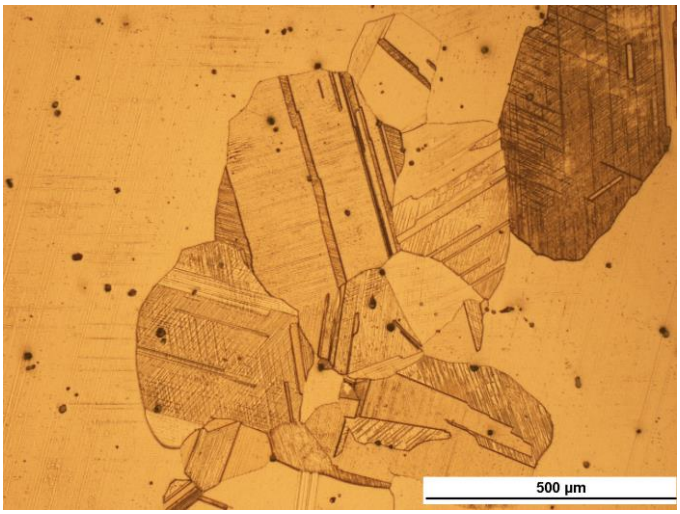

Figure 3. Optical micrograph (100x) - Solution treated Co28Cr22Fe alloy (100 ml HCl + 5 ml H_2O_2)

The X-ray diffraction pattern of the as cast sample (Fig. 4) shows that the specimen consists of a mixture of HCP-ε (Closed-Packed Hexagonal) and FCC-α(Face-Centered Cubic). The volume fraction of the HCP-ε phase is higher than FCC-α. The presence of FCC structure at room temperature indicates a non-equilibrium transformation during cooling. Also in Fig. 4, it is shown the diffraction pattern for an as cast sample after 18 hours of CE testing. After the test, the HCP peaks have a higher intensity and others can be observed, whereas, the FCC peaks have their intensity lowered, that is, during exposure of the surface to cavitation, a strain-induced phase transformation (FCC-α to HCP-ε) occurred. On the other hand, the solution treated sample consists mainly of HCP (Fig. 5). The peak (ε-201) has an intensity 10000 times the others, due to the diffraction of a single hexagonal grain, since the grains are in the order of millimeter.

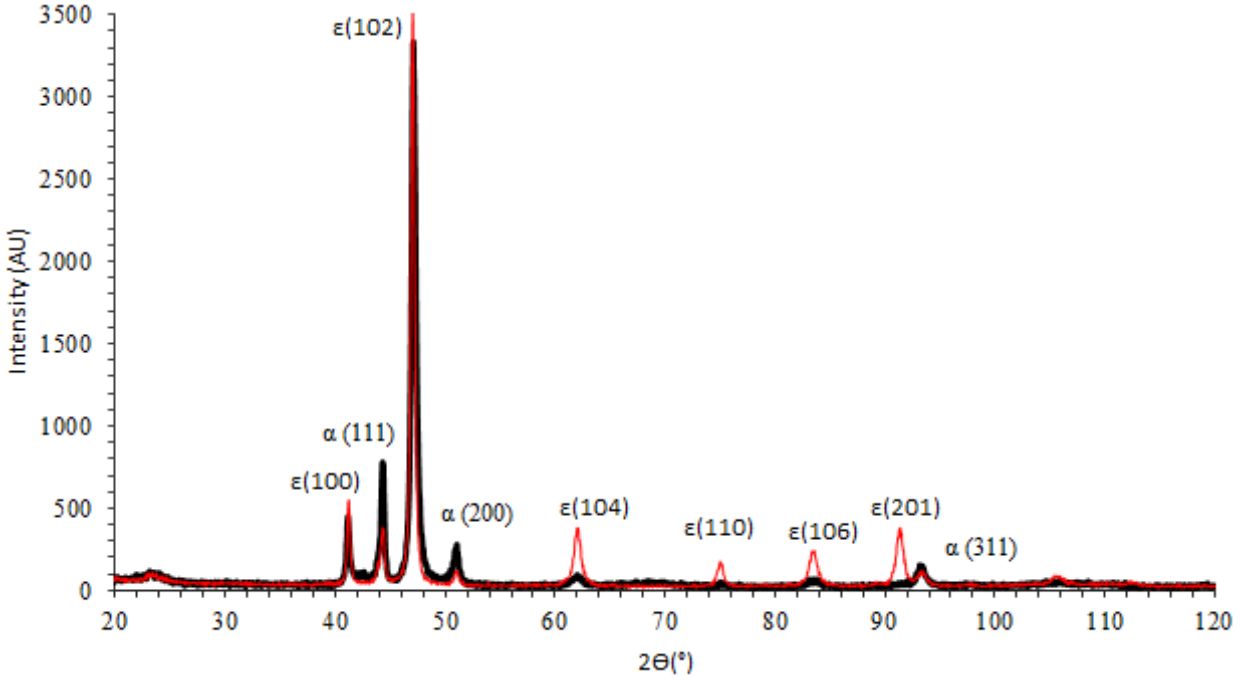

Figure 4. XRD patterns (a) black curve - As cast sample; (b) red curve - As cast after 18 hours CE testing.

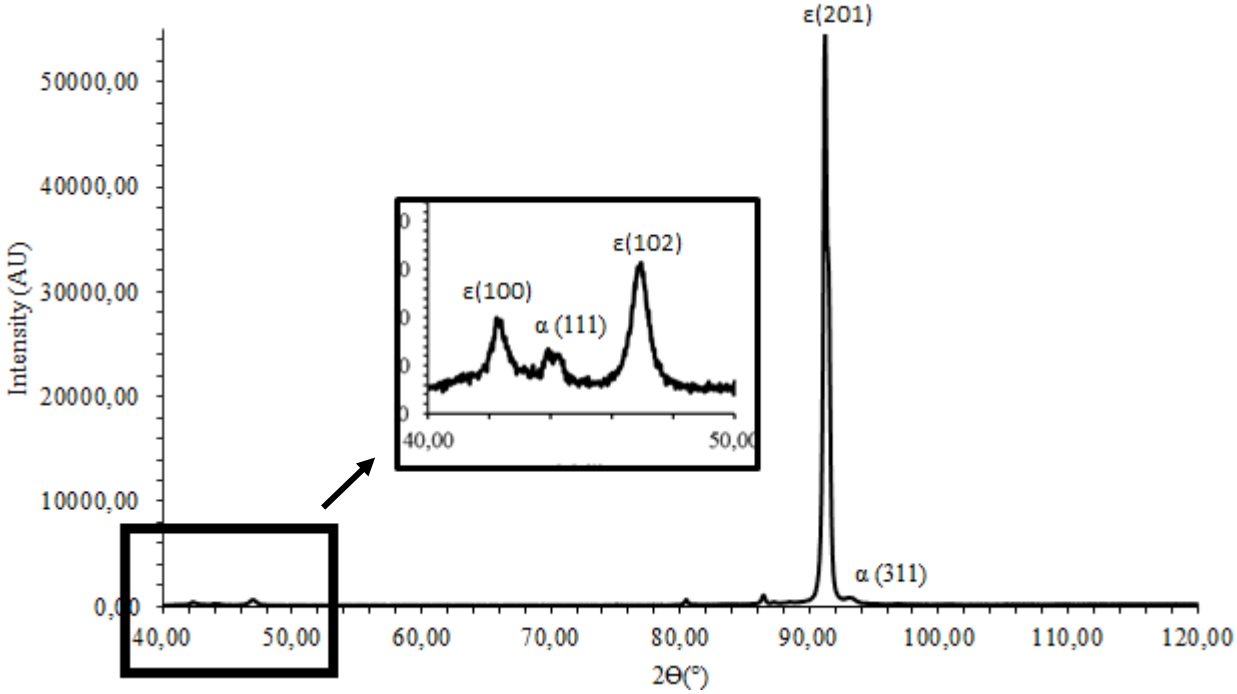

Figure 5. XRD pattern solution treated samples.

Micro hardness results for each condition are shown in Table 3.

Table 3. Microhardness tests results.

Material	Hardness (HV0,1)
Co28Cr22Fe (as-cast)	381±5; 394±8 (Inside deformation twins)
Co28Cr22Fe (solution treated)	345±4 (coarse grains region); 279±3 (recrystallized grains)
Co28Cr22Fe (cold-worked 30%)	384±9

3.2 CE tests

Figure 6 presents the cumulative mass loss as a function of testing time. The curves are divided in two stages, an incubation period with no or very little mass loss, and a damage period, where the cumulative mass loss increases with the exposure time. The three studied conditions showed a higher CE resistance when compared to AISI 304. Solution treated and as-cast samples have the same incubation time (11 hours), which is 4 times the incubation period of AISI 304, but different cumulative mass losses, the as cast showed a total mass loss 49% lower. These results can be attributed to the presence of annealing twins inside the grains, since these are a preferential local for initiating CE damage. Moreover, during CE, a phase transformation from alpha FCC to epsilon HCP occurred, allowing a greater absorption of the cavitation impact energy. On the other hand, the solution treated specimens cannot absorb the impact energy, considering their hexagonal structure.

Cold-worked samples have the longest incubation period (14 hours), and the lowest total mass loss (3 mg), due to a greater difficulty to undergo plastic deformation.

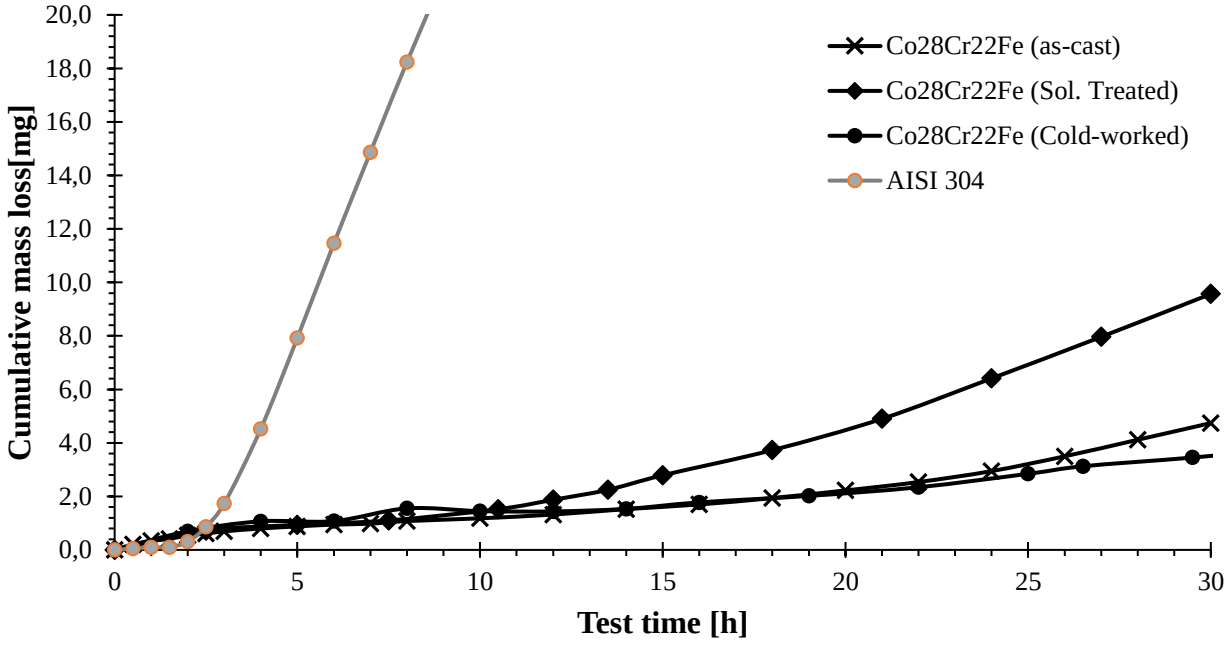

Figure 6. Cumulative mass loss *versus* exposure time

3.3 Scanning electron microscopy of eroded surfaces

Figure 7 shows the cavitation erosion damage on the surface of the as cast Co28Cr22Fe alloy. During the incubation time, plastic flow occurs without mass loss (Fig 7.a). Afterwards, material removal occurs by flaking, starting on slip lines and slip lines intersections (Fig 7.b). Figure 8 shows the eroded surface of the solution treated sample, after 9 hours of CE testing. It is possible to see, as before, flaking occuring mainly at slip lines intersections (Fig. 8.a.), but also at twin boundaries (Fig. 8.b).

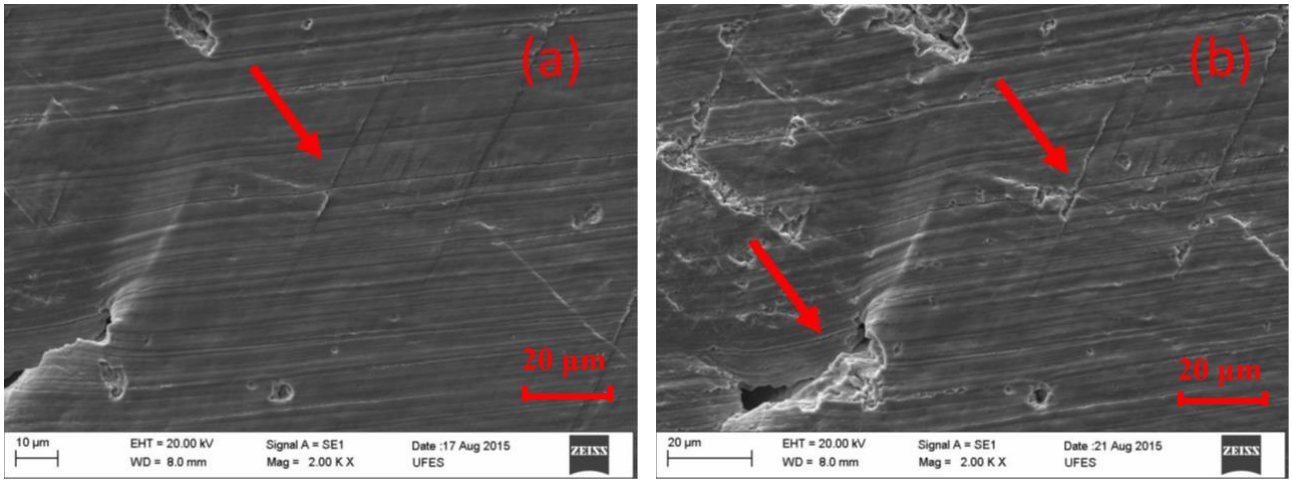

Figure 7. SEM micrograph - Slip lines evolution. Test time (a) 6 hours – Plastic flow without mass loss (extruded slip slines) (b) 12 hours – Flaking occured on slip lines and slip lines intersections.

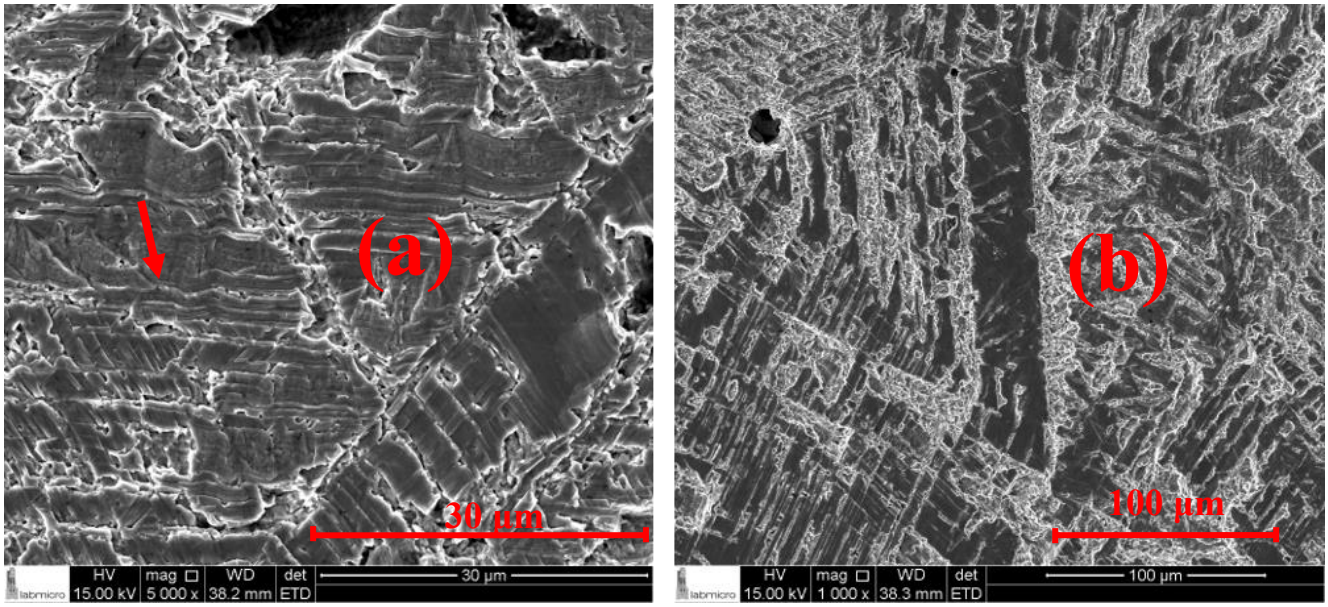

Figure 8. SEM micrograph - Test time 9 hours. Flaking from (a) slip lines intersections and slip lines extrusion (b) twin boundaries – the boundary is eroded while in the interior occurred only plastic flow.

4. CONCLUSIONS

1. Cold-working significantly improves CE resistance of Co28Cr22Fe alloy;
2. Solution treated samples have the same incubation time as the as-cast samples, but significantly different wear rates;
3. The onset of CE damage on cobalt alloys samples occurred preferentially at slip lines.

5. REFERENCES

Gould, G.C., 1980. "The role of mechanical properties in cavitation erosion resistance". In *American Society Testing Materials*, Vol. 474, p. 182.

Hansson, C. and Hansson, L.H., 1992. *Cavitation Erosion*. ASM Handbook, Vol. 18, p.214-220.

Hattori, S. and Mikami, N., 2009. *Cavitation erosion resistance of stellite weld alloy overlays*. Wear, Vol. 267, p. 1954-1960.

Heathcock, C.J., Ball, A., and Protheroe, B.E., 1982. *Cavitation erosion of cobalt-based alloys, cemented carbides and surface-treated low alloys steels.* Wear, Vol. 74, p. 11-26.

Jean, P. and Jean, M., 2005. *Fundamentals of Cavitation*. New York: Kluwear academic publishers.

Mesa, D.H, Tschiptschin, A.P. and Pinedo, C.E., 2006. *On the formation of expanded austenite during plasma nitriding of an AISI 316L austenitic stainless steel.* Surface Coatings and Technology, Vol. 201, p. 1552-1556.

Mills, D.J. and Knutsen, R.J., 1998. *An investigation of the tribological behavior of high-nitrogen Cr-Mn austenitic stainless steel.* Wear, Vol. 215, p. 83-90.

Richman, R.H. and McNaughton, P., 1990. *Correlation of cavitation erosion behavior with mechanical properties of metals.* Wear, Vol. 140, p. 63-83.

Romo, S.A., Fanta, J.F., Giraldo, J.E. and Toro, A., 2012. *Cavitation at high-velocity erosion resistance of welded Stellite 6 alloy.* Tribology International, Vol. 47, p. 16-24.

Sreedhar, B.K., Albert, S.K. and Pandit, A.B., 2015. *Improving cavitation erosion resistance of austenitic stainless steel in liquid sodium by hardfacing – comparison of Ni and Co deposits.* Wear, Vol. 342-343, p. 92-99.

Stoltz, R.E. and Vander Sande, J.B., 1980. *The effect of nitrogen on stacking faul energy of Fe-Ni-Cr-Mn steels.* Metallurgical Transactions, Vol. 11A, p. 1033.

Vaidya, S., Mahajan, S. and Preece, C.M., 1980. *The Role of Twinning in the Cavitation Erosion of Cobalt Single Crystals.* Metallurgical Transactions, Vol. 11A, p. 1139.

Vaidya, S. and Preece, C.M., 1978. *Cavitation erosion of age-hardenable aluminium alloys.* Metallurgical Transactions, Vol.9A, p. 299.

6. RESPONSIBILITY NOTICE

The authors are the only responsible for the printed material included in this paper.